

## Calculated thermodynamic properties of plutonium metal

This article has been downloaded from IOPscience. Please scroll down to see the full text article.

2003 J. Phys.: Condens. Matter 15 8377

(<http://iopscience.iop.org/0953-8984/15/49/015>)

View [the table of contents for this issue](#), or go to the [journal homepage](#) for more

Download details:

IP Address: 171.66.16.125

The article was downloaded on 19/05/2010 at 17:51

Please note that [terms and conditions apply](#).

# Calculated thermodynamic properties of plutonium metal

G Robert<sup>1</sup>, A Pasturel<sup>2</sup> and B Siberchicot<sup>1</sup>

<sup>1</sup> CEA-DIF Département de Physique Théorique et Appliquée, BP 12, 91680 Bruyères-le-Châtel, France

<sup>2</sup> Laboratoire de Physique Numérique, CNRS, 25 avenue des Martyrs, BP 166 CNRS, F-38042 Grenoble Cedex 09, France

E-mail: gregory.robert@cea.fr

Received 8 August 2003

Published 25 November 2003

Online at [stacks.iop.org/JPhysCM/15/8377](http://stacks.iop.org/JPhysCM/15/8377)

## Abstract

In the framework of density functional theory and the generalized gradient approximation, we investigate the effects of magnetism on four plutonium allotropes. We show that an antiferromagnetic configuration gives a structural hierarchy which is consistent with experimental features. Using a simple Debye–Grüneisen model and a corrective term, we are able to draw a  $P$ – $T$  phase diagram of Pu. Harmonic contributions are not sufficient for obtaining a correct description of the thermal properties of Pu and we emphasize the important role played by electronic and anharmonic contributions.

## 1. Introduction

Plutonium metal is one of the most complex of all elements. At ambient pressure Pu transforms into a succession of six crystallographic allotropes from room temperature up to the solid–liquid transition just above 913 K ( $\alpha$ ,  $\beta$ ,  $\gamma$ ,  $\delta$ ,  $\delta'$  and  $\epsilon$  phases). Plutonium melts at a much lower temperature than its neighbours in Mendeleev's table and does so with a decrease in volume. Its phases present very different structures and properties. Some have complex open structures ( $\alpha$  and  $\beta$ : monoclinic) and others close-packed structures, sometimes distorted, ( $\gamma$ : orthorhombic;  $\delta$  and  $\epsilon$ : cubic;  $\delta'$ : tetragonal) [1]. Most unusual is the extreme variation in atomic volume found in plutonium with a 24% volume increase in going from the  $\alpha$  to the  $\delta$  phase.

The reason for the peculiar physical and chemical properties of plutonium lies in its special location in the actinides series, at the boundary between the light actinides which present 5f delocalized states (Th–Np) and the heavy actinides (Am–Lr) with 5f localized states. According to the allotrope, the character of the 5f electrons varies from nearly delocalized, in  $\alpha$ -Pu, to varying degrees of localization, in the other phases. Then, according to the phase,

there is a competition between localization and delocalization of 5f electrons and the behaviour of plutonium is close to those of light or heavy actinides.

It is well known that standard density functional theory (DFT) with some local density approximation (LDA) for the electron exchange and correlation effects fails to reproduce plutonium equilibrium properties. Numerous approaches have been used to go beyond the LDA and recently the LDA +  $U$  approach has been successfully applied to the problem [2, 3]. Nevertheless, as the  $U$  parameter is adjustable, it has been defined for the peculiar case of  $\delta$ -Pu. As the degree of localization of 5f electrons changes in an unknown manner from one phase to another, the value of  $U$  should not be unique and such a method would involve a different value of  $U$  for each allotrope. Then energy differences should no longer be comparable and the LDA +  $U$  approach could be difficult to use for the determination of the whole phase diagram of Pu. Recently the equilibrium properties of  $\delta$ -Pu have also been correctly reproduced by Savrasov *et al* [4] within a dynamical mean-field theory using the same Hubbard parameter. Petit *et al* [5] used self-interaction-corrected (SIC) LDA to study the structural and electronic properties of  $\delta$ -Pu but they obtained a 30% too large equilibrium volume.

In addition to these specific treatments of 5f electron correlations, different kinds of approximation have been successfully taken into account, e.g. the inclusion of magnetism in calculations. Some results have been obtained by Antropov *et al* [6] and Nordström and Singh [7] by considering various atomic non-collinear magnetic configurations. More recently, important results have been obtained by Wang and Sun [8] on  $\delta$ -Pu and  $\epsilon$ -Pu. By using the generalized gradient approximation (GGA) and by considering an antiferromagnetic (AFM) alignment of spins, they reproduced the correct equilibrium volume and an improved bulk modulus.

Other works gave confirmations [9, 10]. Models for disordered local moments (DLM) have also been successfully applied from thorium to californium [11]. More particularly, Söderlind *et al* [10] investigated several magnetic configurations including DLM; the most energetically favourable structures were obtained for the AFM type-I ordering and random ordering in  $\delta$ -Pu. They consider also that magnetic interactions can be used to calculate the transition between the  $\delta$  and  $\gamma$  phases [12].

The case of AFM  $\alpha$ -Pu has also been investigated by Kutepov *et al* [13]. Very recently, we showed that such GGA magnetism-based calculations are able to reproduce the high negative values of the formation energies of  $\text{Pu}_{(1-x)}\text{M}_x$  ( $\text{M} = \text{Al}, \text{Ga}$  and  $\text{In}$ ) [14] compounds.

This quantity of coherent results indicates the important role played by magnetic interactions, especially in the formation of local magnetic moments, in electronic structure and in the stability of some of the plutonium phases. Although there is no direct experimental evidence of magnetic moments in plutonium, some hypotheses can be advanced regarding possible spin-glass-like or spin-fluctuation behaviours [13] for this metal.

In this paper, we apply the GGA AFM approximation in order to determine the ground state properties of plutonium allotropes. In a second step, an appropriate thermodynamic model is discussed, in order to expand our results as a function of temperature and pressure. Then the solid part of the Pu phase diagram is obtained.

In section 2 the details of the electronic structure calculations are presented. The thermodynamic model and results are described in section 3 and section 4 contains the results and a discussion of them. A summary and the conclusions of this work are given in section 5.

## 2. Computational details

The electronic structure calculations are based on the all-electron full-potential linear augmented plane-wave (FP-LAPW) method [15]. The self-consistent calculations are

**Table 1.** Equilibrium volumes, bulk moduli and energy differences for five phases of Pu. The minimum energy of the  $\alpha$  AFM structure is the reference. The experimental values come from [1].

Phase	Approximation used	$V_0$ (Å <sup>3</sup> /atom)	$B_0$ (GPa)	Minimum energy (mRyd)
$\alpha$	Non-spin-polarized	18.10	169.2	1.8
$\gamma$	Non-spin-polarized	18.20	129.2	27.4
$\delta$	Non-spin-polarized	19.57	99.9	48.7
$\delta'$	Non-spin-polarized	19.53	98.5	47.4
$\epsilon$	Non-spin-polarized	17.69	144.1	28.1
$\alpha$	Spin-polarized AFM	18.47	101.1	0
$\gamma$	Spin-polarized AFM I	22.14	35.2	13.3
$\gamma$	Spin-polarized AFM II	21.90	44.4	8.0
$\delta$	Spin-polarized AFM	23.43	54.8	9.0
$\delta'$	Spin-polarized AFM	23.13	55.4	8.8
$\epsilon$	Spin-polarized AFM	21.19	45.1	12.9
$\alpha$	Experimental	19.90	55.9	—
$\gamma$	Experimental	23.14	22.7	—
$\delta$	Experimental	24.92	33.9	—
$\delta'$	Experimental	24.76	—	—
$\epsilon$	Experimental	24.04	—	—

performed with a fully relativistic treatment of electrons in core states and a scalar-relativistic treatment including spin-orbit coupling (SOC) for the valence electrons. Additional  $p_{1/2}$  local orbitals (LO) are included in the basis set in order to treat the 6p semi-core states modified by SOC accurately [16]. The GGA [17] is used and magnetic configurations are taken into account. The basis sets include the 6s, 6p, 7s, 7p, 6d and 5f partial waves.

Moreover, in order to obtain more flexibility in the radial basis functions and to decrease the basis set size, new LO (APW + lo) for 5f partial waves of Pu are included [18].

All structures have been calculated with a muffin-tin radius of 2.5 bohrs except for the  $\alpha$  phase (2.1 bohrs). This difference in radius is related to the distance between first-neighbour atoms in this peculiar structure. Nevertheless, the choice of the muffin-tin radius does not modify our results. For instance using 2.1 bohrs for the  $\delta$  phase leads to a variation of the cohesive energy smaller than 0.3 mRyd/atom. The change of the equilibrium volume is less than 0.5%. Finally we used  $k_{\max} R_{\text{mt}} = 10$  for plane-wave convergence (where  $R_{\text{mt}}$  is the atomic sphere radius,  $k_{\max}$  is the plane-wave cut-off) and the cut-off energy in the second variational step equals 4.5 Ryd for SOC.

### 3. Structural stabilities and equations of state at 0 K

The structures of interest in this study are the monoclinic  $\alpha$  structure, the body-centred orthorhombic  $\beta$  structure, the face-centred cubic  $\delta$  structure and the body-centred cubic  $\epsilon$  structure. The  $\gamma$ - $\epsilon$  transition occurs by way of an intermediate body-centred tetragonal  $\gamma'$  phase, which exists only in a very narrow temperature interval. For the  $\alpha$ ,  $\delta$  and  $\epsilon$  phases, our calculations lead to results in close agreement with previous calculated equations of state (EOS) [8, 10, 13]. Equilibrium properties and energy differences are reported in table 1.

It seems clear from table 1 that non-spin-polarized calculations fail to reproduce equilibrium volumes and bulk moduli. The calculated energy differences between the different phases show that the  $\alpha$  phase is the most stable structure. However, these energy differences are too high to be consistent with the experimental transition temperatures.

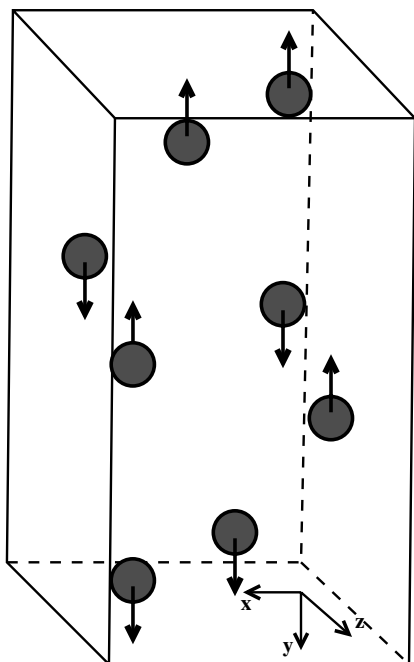


**Figure 1.** Antiferromagnetic configuration type I for the  $\gamma$  phase.

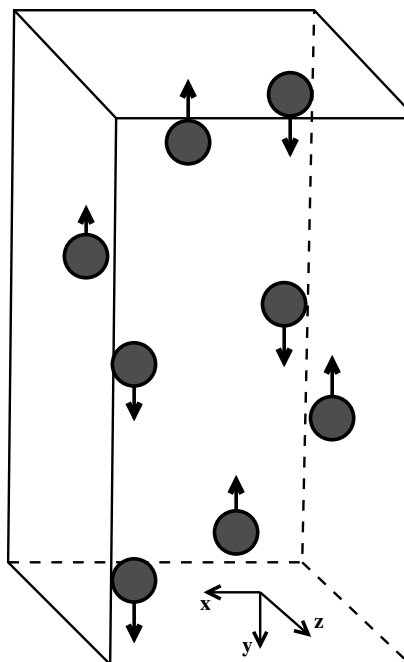


**Figure 2.** Antiferromagnetic configuration type II for the  $\gamma$  phase.

For spin-polarized calculations, the appearance of magnetic moments in Pu compounds for increasing volumes could be related to Hill's considerations [19]. In this model the 5f electron correlations lead to a close relationship between magnetic properties and Pu–Pu distances. Thus for internuclear distances larger than 3.4 Å, plutonium atoms could bear a magnetic moment. For all allotropes considered except for the  $\alpha$  phase ( $\simeq 2.3$  Å at equilibrium volume), our ferromagnetic calculations present such a magnetic transition at Pu–Pu distances around 3.0 Å. Consequently, two minima in the energy–volume curves are observed for  $\gamma$  and  $\epsilon$  structures.

Taking into account an AFM configuration leads to strong changes in EOS of these structures, as seen in table 1. Equilibrium volumes and bulk moduli are in better agreement with experimental features and can be compared to LDA +  $U$  calculations for the  $\delta$  phase [2]. These effects result from a band splitting as compared to the GGA non-magnetic calculations and a partial localization of 5f electrons which reduce the chemical bonding. This leads to an increased equilibrium volume and a reduced bulk modulus. Let us point out that a LAPW treatment of the complex body-centred monoclinic structure of the  $\beta$  phase (34 atoms per unit cell) is too computer-time-consuming and the study of its magnetic configurations cannot be included in this contribution.

From an energetic point of view,  $\delta$  and  $\delta'$  structures are the most strongly affected phases followed by the  $\gamma$  and  $\epsilon$  phases. The  $\gamma$  AFM phase shows two behaviours depending on the magnetic configuration. AFM type-II-like structure is more stable than AFM type-I structure (figures 1, 2). AFM type-II structure is not a layer of up and down spins but can be considered as a more disordered magnetic structure. Another point is that the energy of the  $\alpha$  phase is less affected by magnetism. Although only one peculiar AFM configuration has been considered (figure 3), the effect of magnetism does not lead to important changes of the EOS or energy.

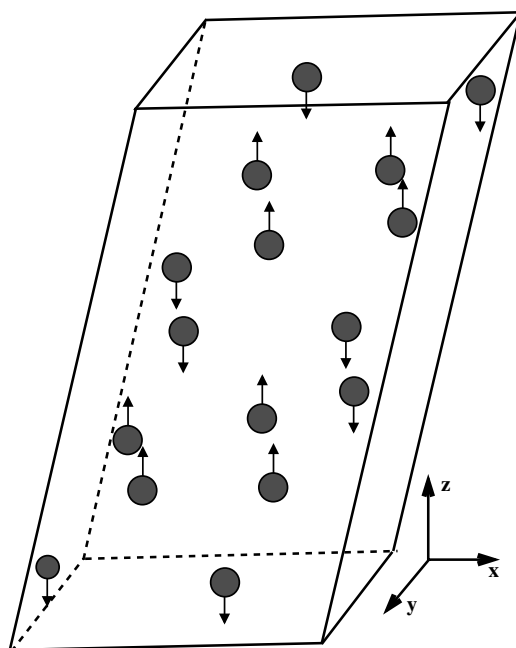


Figure 3. The antiferromagnetic configuration of the  $\alpha$  phase.

By using a different magnetic configuration, Kutepov *et al* [13] find a similar behaviour of this phase.

It is important to note that AFM GGA calculations lead to a structural hierarchy in qualitative agreement with experimental results. The  $\alpha$  phase is the most stable structure, followed by  $\gamma$ ,  $\delta$  and  $\delta'$  (which can be considered as degenerate in energy) and  $\epsilon$  phases. Another interesting point is that the energy differences between these structures are not so far from the values obtained by Wallace [20] who determines the EOS of the different phases by fitting the experimental phase diagram (see figure 4). However, let us emphasize that the small energy difference between the  $\delta$  and  $\delta'$  phases is not reproduced in our calculations and the calculated energy differences between the  $\alpha$  phase and the high-temperature phases seem to be too large.

To illustrate the dominant role played by magnetic interactions, we have explored the Bain path of Pu. In plutonium, the transition  $\delta$ - $\delta'$ - $\epsilon$  can be viewed as the deformation of a tetragonal structure with the values of the tetragonal parameter  $c/a = 1.41$ , 1.33 and 1.0 respectively. We have performed a study of the energy variation as a function of the  $c/a$  ratio for three different volumes. The results are shown in figure 5. We can see that spin-polarized AFM calculations predict two minima in the Bain paths. One minimum is for a tetragonal structure with  $c/a = 0.85$  and is volume independent. The second minimum occurs at a  $c/a$  value which depends on the volume. At the experimental equilibrium volume of  $\delta$ -Pu, this second minimum corresponds to  $c/a = 1.41$ . At lower volume, this minimum occurs at a  $c/a$  value close to the value 1.33 found for the  $\delta'$  structure.

Thus our results predict instability of the  $\delta$  phase at the calculated equilibrium volume (23.43 Å) and stability for expanded volumes. This behaviour of  $\delta$ -Pu is in agreement with the work of Söderlind *et al* [10] who also found that  $\delta$ -Pu is unstable at the calculated equilibrium volume.

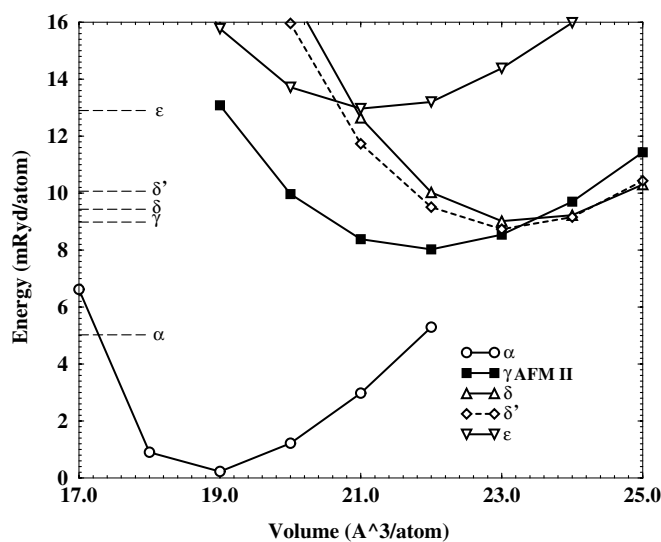


**Figure 4.** The energy–volume curve for Pu in the AFM configuration. Dashed lines on the left are energy differences obtained by Wallace [20].

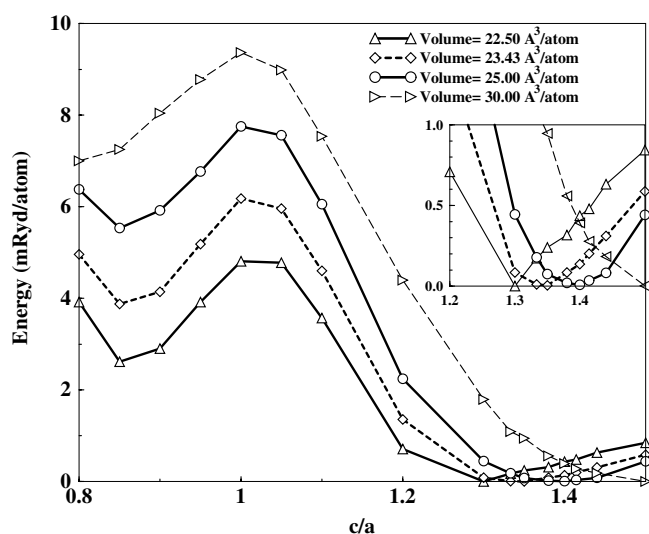


**Figure 5.** The Bain paths for Pu in the AFM configuration.  $c/a = \sqrt{2}$  and  $c/a = 1$  correspond to  $\delta$  and  $\epsilon$  structures respectively. The inset is an enlargement near the  $c/a = \sqrt{2}$  region.

We have calculated the elastic constants  $C'$  of the  $\delta$  and  $\epsilon$  phases at their experimental equilibrium volumes (table 2). The calculated  $C'$  value of  $\delta$  is found to be in good agreement with the measured value [22]. However, the small value of  $C'$  implies a soft response of the system to volume-conserving tetragonal distortion as discussed above. The  $C_{44}$  calculation for the AFM configuration requires a superstructure in order to keep the same magnetic neighbouring and was not calculated. On the other hand, the bcc structure is located at a maximum and so is not stabilized. As emphasized by Dai *et al* [21], the vibrations in this

**Table 2.** Elastic constants in GPa. The experimental values come from [22].

Phase	Approximation used	$B_0$	$(C_{11} - C_{12})/2$	$C_{11}$	$C_{12}$	$C_{44}$
$\delta$	Non-spin-polarized	99.9	-49.5	—	—	—
$\delta$	Spin-polarized AFM	54.8	10.6	68.9	47.7	—
$\epsilon$	Non-spin-polarized	144.1	57.6	220.9	105.7	-6.2
$\epsilon$	Spin-polarized AFM	45.1	-29.1	—	—	—
$\delta$	Experimental	33.9	4.78	36.28	26.73	33.59

phase are extremely anharmonic and this results in a soft phonon spectrum which is only stable at high temperatures.

The general agreement between the experimental results, calculated EOS and structural hierarchy encourages us to calculate the thermodynamic properties of plutonium metal in the framework of a Debye model.

#### 4. The thermodynamic model and results

Phase diagrams typically display phase stability as a function of temperature and pressure. As phonon spectra calculations are very complex to perform in the case of multiple plutonium allotropes, we choose a simpler way to investigate the structural phase transitions on the basis of first-principles bonding curves and the use of the Debye–Grüneisen theory. Let us consider a system with a given averaged atomic volume  $V$  and temperature  $T$ . The Helmholtz free energy  $F(V, T)$  can be written as a sum of different contributions:

$$F(V, T) = E_c(V) + F_{\text{ion}}(V, T) + F_{\text{el}}(V, T) + F_{\text{mag}}(V, T) + F_{\text{AE}}(V, T) \quad (1)$$

where  $E_c$  represents the 0 K total energy,  $F_{\text{ion}}$  the vibrational free energy of the lattice,  $F_{\text{el}}$  the free energy due to the thermal excitation of electrons,  $F_{\text{mag}}$  the magnetic free energy [8] and  $F_{\text{AE}}$  an additional empirical term describing anharmonic effects [20].

Within the Debye–Grüneisen model, the lattice can vibrate at all frequencies up to a Debye cut-off frequency  $\omega_D$  defined by

$$\frac{h}{2\pi}\omega_D = k_B\Theta_D \quad (2)$$

where  $h$  and  $k_B$  are the Planck and Boltzmann constants.  $\Theta_D$  is the Debye temperature. Assuming a constant sound velocity, it can be expressed as [23]

$$\Theta_D = K \left[ \frac{aB}{M} \right]^{1/2} \quad (3)$$

where  $a$  is the lattice constant (au),  $B$  the bulk modulus (kbar) and  $M$  the mass (au).  $K$  is a constant mainly depending on the crystallographic structure.

For cubic metals, the universal  $K$  value is 26.024 and reproduces quite well the Debye temperature of different elements [24]. The simplest way to define the numerical value of  $K$  for non-cubic metals is by using relation (3) with the experimental  $\Theta_D$  and  $B$ . Using experimental results from [1, 25], we obtain  $K = 35.056$  for the  $\alpha$  phase and  $K = 28.360$  for the  $\delta$  phase. This last value is close to the universal  $K$ . As the Debye temperatures are not known for the two remaining structures ( $\gamma$  and  $\epsilon$ ) we use the values of  $K = 28.360$  for these phases since  $\epsilon$  is a cubic phase and  $\gamma$  can be considered as close to a close-packed cubic structure. Finally, we use these  $K$  values with the calculated bulk modulus in order to determine theoretical Debye temperatures. Then the differences between the experimental and calculated Debye



temperatures are due to errors produced in the calculation of the bulk modulus. Let us note that this error is less than 5% of the experimental Debye temperature for the  $\delta$  phase.

The Debye temperature varies with temperature and anharmonic effects in the vibrating lattice are described in terms of a Grüneisen constant  $\gamma$ . The vibrational free energy and entropy can be written as

$$E_D(V, T) = \frac{9}{8}Nk_B\Theta_D + 3Nk_BTD(\Theta_D/T) \quad (4)$$

and

$$S_D(T) = 3k_B[\frac{4}{3}D(\Theta_D/T) - \ln(1 - e^{-\Theta_D/T})] \quad (5)$$

where  $D(\Theta_D/T)$ , the Debye function, varies from unity at high temperature to zero at low temperature.

Neglecting electron–phonon interactions, the electronic contribution to the free energy is  $F_{el} = E_{el} - TS_{el}$  where

$$E_{el}(V, T) = \int n(\varepsilon, V)f\varepsilon d\varepsilon - \int^{\varepsilon_F} n(\varepsilon, V)\varepsilon d\varepsilon \quad (6)$$

and

$$S_{el}(V) = -k_B \int n(\varepsilon, V)[f \ln f + (1 - f) \ln(1 - f)] d\varepsilon \quad (7)$$

where  $n(\varepsilon, V)$  is the electronic density of states and  $f$  is the Fermi distribution.

In the framework of our calculations, we considered plutonium as an AFM metal. Following [8] we introduce a magnetic entropy term:

$$F_{mag}(V, T) = -k_B T \ln[M_s(2L - M_s) + 1] \quad (8)$$

where  $F_{mag}(V, T)$  is the energy of the magnetic entropy,  $M_s$  is the total spin moment and  $L$  is the 5f orbital moment.

Finally, the last term in the expression for the energy is the anharmonic free energy due to phonon–phonon interactions and non-adiabatic effects of electron–phonon interactions. We used the empirical relation introduced by Wallace [20]:

$$F_{AE}(V, T) = -D(V, T)T^2. \quad (9)$$

We are now ready to shed light on the thermodynamics of the different phase transitions of Pu, stressing the importance of the different contributions to the Helmholtz free energy. As regards the vibrational contribution, it is noteworthy that the thermal expansion coefficient is positive in a Debye model and cannot reproduce the experimental specificity for the  $\delta$  phase. Moreover, it is known [21] that the  $\epsilon$  phase presents a strong anharmonic character. Therefore it will be necessary to use different values of  $F_{AE}$  as discussed below. Despite these considerations, the set of calculated Debye temperatures, i.e. 203, 112, 126 and 112 K for the  $\alpha$ ,  $\gamma$ ,  $\delta$  and  $\epsilon$  phases respectively, ensures that the harmonic contribution is the most important contribution to the thermal free energy. To make this notion quantitative, let us note that this term represents more than 60% of the thermal part of the Helmholtz free energy difference at each transition temperature studied.

Accurate evaluation of electronic free energies is another problem. Although the calculated specific heat for the  $\alpha$  phase is rather close to the experimental value, it is more difficult to reproduce this quantity for the  $\delta$  phase due to the experimentally narrow peak observed in the DOS at the Fermi level [26]. The electronic structure of  $\delta$ -Pu is strongly modified within the spin-polarized calculations compared to the LDA calculations as mentioned in [10] and [11]. Spin-polarized calculations improve the agreement with the experimental photoelectron spectrum but not with an accuracy which allows a quantitative treatment. Indeed

**Table 3.** The equivalence of the  $D$  terms ( $10^{-9}$  Ryd  $\text{K}^{-2}$ ) of the free electronic energies calculated with the Sommerfeld model and equations (6), (7).

Phase	$F_{\text{elec}}$		$F_{\text{elec}}$
	$F_{\text{elec}}$	approximated with $N(E)$ <i>ab initio</i>	
$\alpha$	-2.75	-2.37	-6.48
$\gamma$	-3.58	-2.79	
$\delta$	-3.55	-3.72	-24.38
$\epsilon$	-3.58	-3.35	

**Table 4.** Values of the  $D$  term ( $10^{-9}$  Ryd  $\text{K}^{-2}$ ).

Phase	$F(V, T)$
$\alpha$	0
$\gamma$	-25.74
$\delta$	-32.32
$\epsilon$	-36.75

if the small spectral weight of the narrow peak leads to weak effects on the energy differences it can become important to describe the thermal excitation of the electrons. In order to estimate the relative importance of this effect, we calculate the electronic contributions for the  $\delta$  and  $\alpha$  phases from equations (6), (7) and from the Sommerfeld model with the theoretical specific heat. The first result is that the electronic contributions are very close whatever the allotrope and the method used to calculate them (see table 3). If we now use the Sommerfeld model with the experimental specific heats [25] of  $\alpha$ -Pu and  $\delta$ -Pu, the discrepancy found for  $\delta$ -Pu confirms the important role played by the narrow peak.

The magnetic contribution is related to the choice of the AFM configuration for all the allotropes studied. Therefore this term will make a negligible contribution since the magnetic moments do not differ very much from one structure to another. Let us note that a more complex magnetic order could appear at high temperatures which could give more weight to the magnetic contribution [12].

The anharmonic term  $D$  is approximated in such a way that the different experimental transition temperatures are reproduced at ambient pressure: 417 K for  $\alpha \rightarrow \gamma$ , 590 K for  $\gamma \rightarrow \delta$  and 725 K for  $\delta \rightarrow \epsilon$ . We suppose that the  $\alpha$  phase is correctly reproduced without anharmonicity ( $D = 0$ ). The values of  $D$  are given in table 4. At the  $\alpha \rightarrow \gamma$  transition, this corrective term represents 25% of the total temperature contribution to the free energy of the  $\gamma$  phase, 30% for  $\gamma$  and  $\delta$  structures at 590 K ( $\gamma \rightarrow \delta$ ) and near 40% for the  $\delta$  and  $\epsilon$  phases at 725 K ( $\delta \rightarrow \epsilon$ ).

It must be emphasized that, in fact,  $F_{\text{AE}}$  contains not only anharmonic effects but also all the corrections due to the inability of GGA spin-polarized calculations to reproduce some experimental features. This term could be considered as a more general corrective quantity including inaccuracies in 0 K energy differences and bulk moduli and errors in fits, as can be seen from figure 4. Moreover, another part of  $F_{\text{AE}}$  comes from the electronic contribution as discussed above. If we express electronic energies in terms of  $D$  (table 3), the experimental difference between the  $\alpha$  and  $\delta$  phases is  $17.9 \times 10^{-9}$  Ryd  $\text{K}^{-2}$ . This value is greater than half the corrective  $D$  values given in table 4. The  $D$  values for the two remaining structures ( $\gamma$  and  $\epsilon$ ) are close to that of the  $\delta$  phase. The smaller value obtained for the  $\gamma$  phase may be due to the electronic energy loss in going from  $\delta$  to the  $\gamma$  phase with its slightly smaller volume. For the  $\epsilon$  phase, this electronic energy loss is largely compensated by important anharmonic effects.

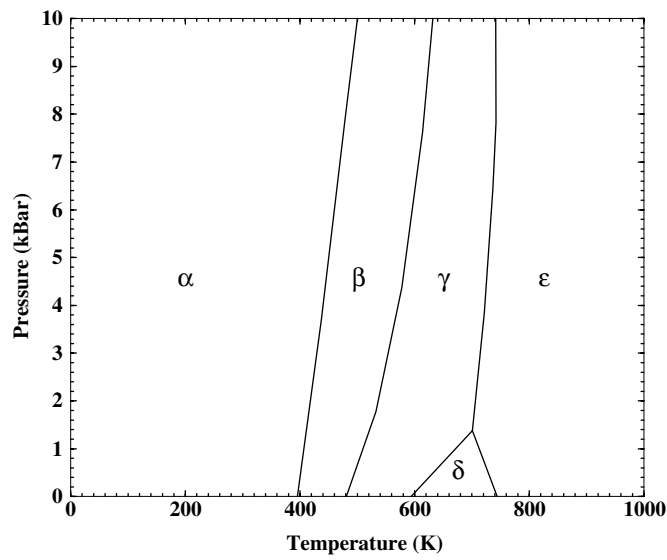


Figure 6. The experimental phase diagram obtained by Stephens [27].

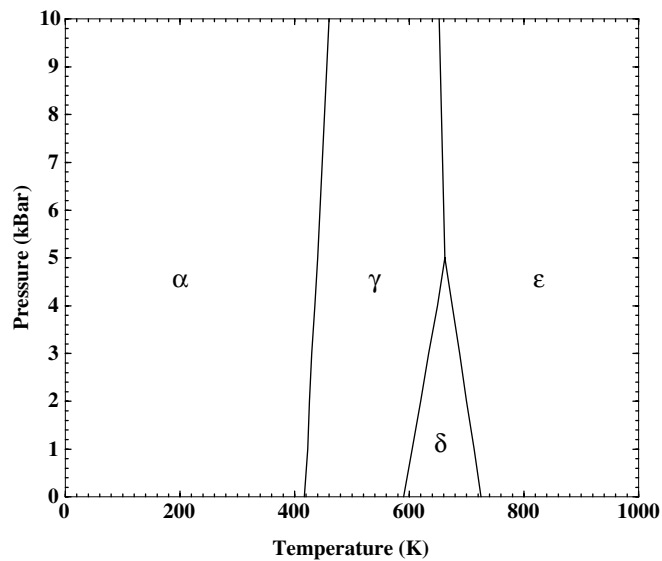


Figure 7. The calculated phase diagram.

Despite some crude approximations, we calculate the Gibbs energies of this system for different pressures. Then it is possible to obtain the solid part of the Pu phase diagram including  $\alpha$ ,  $\gamma$ ,  $\delta$  and  $\epsilon$  structures (figures 6, 7).

## 5. Conclusions

To conclude, we have tried to demonstrate the possibility of calculating the  $P$ - $T$  phase diagram of Pu within the framework of a rather simple Debye model. At  $T = 0$  K, only GGA

spin-polarized calculations are able to give energy differences between the different allotropes which are consistent with the gross features of the experimental phase diagram of Pu. We show also that the  $\varepsilon$  phase is mechanically unstable while the small positive value of  $C'$  for the  $\delta$  phase calculated at the experimental volume implies a soft response of the system to volume-conserving tetragonal distortion. Harmonic contributions calculated in the Debye model are not sufficient for obtaining a correct description of the thermal properties of different allotropes. More particularly, the electronic contributions for the  $\gamma$ ,  $\delta$  and  $\varepsilon$  phases as well as the anharmonic contribution for the  $\varepsilon$  phase play an important role in determining the transition temperatures. We emphasize that accurately evaluating each of these contributions remains a challenge for the actual DFT-based calculations.

## References

- [1] Wick O J 1980 *A Guide to the Technology (Plutonium Handbook vol 1)* (Lagrange Park, IL: American Nuclear Society)
- [2] Bouchet J, Siberchicot B, Jollet F and Pasturel A 2000 *J. Phys.: Condens. Matter* **12** 1723
- [3] Savrasov S Y and Kotliar G 2000 *Phys. Rev. Lett.* **84** 3670
- [4] Savrasov S Y, Kotliar G and Abrahams E 2001 *Nature* **410** 793
- [5] Petit L, Svane A, Temmerman W M and Szotek Z 2000 *Solid State Commun.* **116** 379
- [6] Antropov V P, Van Schilfgaarde M and Harmon B N 1995 *J. Magn. Magn. Mater.* **140–144** 1355
- [7] Nordström L and Singh D J 1996 *Phys. Rev. Lett.* **76** 4420
- [8] Wang Y and Sun Y F 2000 *J. Phys.: Condens. Matter* **21** L311
- [9] Söderlind P 2001 *Europhys. Lett.* **55** 525
- [10] Söderlind P, Landa A and Sadigh B 2002 *Phys. Rev. B* **66** 205109
- [11] Niklasson M N, Wills J M, Katsnelson M I, Abrikosov I A, Eriksson O and Johansson B 2003 *Phys. Rev. B* **67** 235105
- [12] Landa A, Söderlind P and Ruban A 2003 *J. Phys.: Condens. Matter* **15** L371–6
- [13] Kutepov A L and Kutepova S 2003 *J. Phys.: Condens. Matter* **15** 2607
- [14] Robert G, Pasturel A and Siberchicot B 2003 *Phys. Rev. B* **68** 75109
- [15] Blaha P, Schwarz K, Madsen G, Kvasnicka D and Luitz J 2001 *WIEN2k* (Vienna: Technical University Press)
- [16] Kunes J, Novak P, Schmid R, Blaha P and Schwarz K 2001 *Phys. Rev. B* **64** 153102
- [17] Perdew J P and Singh D J 1992 *Phys. Rev. B* **46** 6671
- [18] Madsen G K H, Blaha P, Schwarz K, Sjöstedt E and Nordström L 2001 *Phys. Rev. B* **64** 195134
- [19] Hill H H 1970 *Plutonium 1970 and Other Actinides* (New York: W M Miner)
- [20] Wallace D C 1998 *Phys. Rev. B* **58** 15433
- [21] Dai X, Savrasov S Y, Kotliar G, Migliori A, Ledbetter H and Abrahams E 2003 *Science* **300** 953
- [22] Ledbetter H M and Moment R L 1976 *Acta Metall.* **24** 891
- [23] Ostanin S A and Trubitsin V Y 1998 *Phys. Rev. B* **57** 13485
- [24] Moruzzi V L, Janak J F and Schwarz K 1988 *Phys. Rev. B* **37** 790
- [25] Lashley J C, Singleton J, Migliori A, Betts J B, Fisher R A, Smith J L and McQueeney R J 2003 *Preprint cond-mat/0306257*
- [26] Arko A J, Joyce J J, Morales L, Wills J, Lashley J, Wastin F and Rebizant J 2000 *Phys. Rev. B* **62** 1773
- [27] Stephens D R 1963 *J. Phys. Chem. Solids* **24** 1197